

# Reversible to Irreversible Transitions in Pattern-Forming Systems with Cyclic Interactions

C. Reichhardt and C. J. O. Reichhardt

*Theoretical Division and Center for Nonlinear Studies,  
Los Alamos National Laboratory, Los Alamos, New Mexico 87545, USA*

(Dated: January 21, 2026)

Transitions from reversible to irreversible or fluctuating states above a critical density and shear amplitude have been extensively studied in non-thermal cyclically sheared suspensions and amorphous solids. Here, we propose that the same type of reversible to irreversible transition occurs for a system of particles with competing short-range attraction and long-range repulsion, which can form crystals, stripes, and bubbles as the ratio of attraction to repulsion varies. By oscillating the strength of the attractive part of the potential, we find that the system can organize into either time-periodic states consisting of nondiffusive complex closed orbits, or into a diffusive fluctuating state. A critical point separates these states as a function of the maximum strength of the attraction, oscillation frequency, and particle density. We also find a re-entrant behavior of the reversible state as a function of the strength of the attraction and the oscillation frequency.

**Introduction**— A non-thermal suspension of colloidal particles under cyclic shear organizes after a number of oscillations into a steady state that can be either reversible, where the particles return to the same positions after each cycle, or irreversible or fluctuating, where the particles undergo diffusion over repeated cycles [1–3]. Above a critical shear amplitude at fixed density or a critical density at fixed shear amplitude, the system remains in an irreversible state, and this critical point is accompanied by a divergence in the number of cycles required for the establishment of a steady state [2–9]. The reversible-irreversible transition is an example of a nonequilibrium absorbing phase transition, and when particle collisions are absent in the reversible state, the transition is referred to as random organization [2, 3, 10]. Similar reversible (R) to irreversible (IR) transitions have also been observed for cyclic shearing of strongly interacting systems, such as amorphous solids, where in the reversible state, the particles return to their original locations after executing complex two-dimensional orbits that may span one or multiple shear cycles [11–19]. Periodically sheared systems that exhibit R-IR transitions additionally show a variety of memory effects [20–24]. R-IR transitions have also been studied for periodically driven systems moving through quenched disorder, such as superconducting vortices with random pinning [25, 26] and colloidal particles in obstacle arrays [27, 28].

An open question is whether similar R-IR transitions can occur for other types of nonequilibrium systems in the absence of periodic shear but the presence of some other type of cyclic driving, such as a periodic oscillation of the pairwise interaction potential between the particles. There are a variety of systems that can be effectively modeled with competing short-range attraction and long-range repulsion (SALR), which form crystal, stripe, labyrinth, void lattice, and bubble states as a function of the ratio of attraction to repulsion or the particle density [29–39]. In a recent experimental realization of a SALR system [39], Hooshanginejad *et al.* could continuously vary the ratio of competing magnetic

and capillary interactions between particles by applying a magnetic field. In SALR systems of this type, it would be possible to cycle the ratio of the attraction to repulsion as a function of time, and see whether the particles settle into a steady state where they return to the same positions after each cycle or remain in a fluctuating or liquid state.

Here, we consider a two-dimensional (2D) system of interacting particles with competing short-range attraction and long-range repulsion, where we cycle the amplitude of the attractive interaction. For a fixed oscillation frequency and particle density, the system always forms a reversible state when the maximum attraction amplitude is weak. We find that there is a critical attraction amplitude above which the system becomes irreversible and displays diffusive behavior similar to that found in cyclically sheared systems. We also find critical oscillation frequencies and particle densities where the system organizes into a reversible state, and near this R-IR transition, the time scale for reaching a steady state diverges as a power law. In the reversible state there can be complex orbits where groups of particles traverse closed loops around patches of particles that remain immobile. At higher densities, dynamical lace-like patterns of motion can appear. The time-periodic reversible states can be regarded as examples of a classical discrete time crystal [40–43]. Our results show that R-IR transitions can be realized by oscillating the interaction potential, rather than by applying a cyclic shear, which could open new ways to study memory and dynamic pattern formation.

**Simulation**— We model a 2D system of size  $L \times L$  with periodic boundary conditions in the  $x$  and  $y$  directions. The system contains  $N$  particles with a density  $\rho = N/L^2$ , and we take  $L = 36$ . The particles have a time-dependent SALR interaction potential of the form

$$V(r_{ij}, t) = \frac{1}{r_{ij}} - B(t) \exp(-r_{ij}) . \quad (1)$$

The distance between particles  $i$  and  $j$  is  $r_{ij} = |\mathbf{r}_i - \mathbf{r}_j|$ , and  $B$  is the strength of the attraction. The long-range

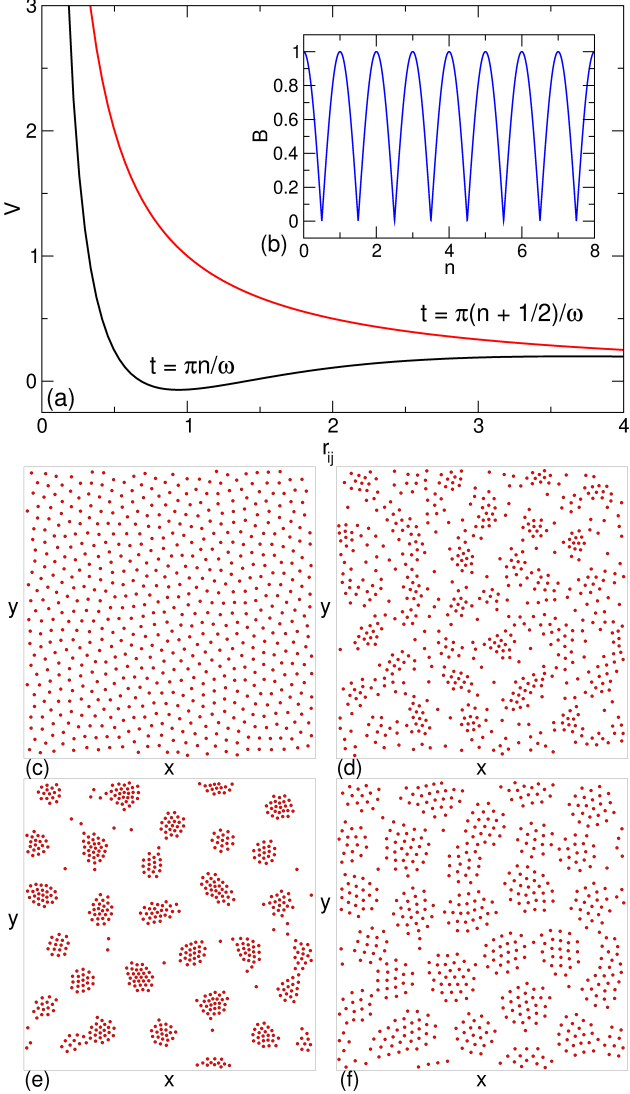


FIG. 1. (a) The SALR interaction potential  $V(r_{ij}, t) = 1/r_{ij} - B(t) \exp(-r_{ij})$  for  $B_{\max} = 2.9$  and  $\omega = 1.25 \times 10^{-4}$  at two different times,  $t = \pi n / \omega$  (black) where  $B(t) = B_{\max}$  and  $t = \pi(n + 1/2) / \omega$  (red) where  $B(t) = 0$  and the interaction is purely repulsive. (b) The corresponding short range interaction strength  $B(t) = B_{\max} |\cos(\omega t)|$  plotted against cycle number  $n$ . (c-f) Particle configurations for a system with  $B_{\max} = 2.9$ ,  $\rho = 0.5$  and  $\omega = 1.25 \times 10^{-4}$  during cycle  $n = 20$ . (c) Uniform state at  $B/B_{\max} = 0.0$ . (d) Beginning of bubble formation at  $B/B_{\max} = 0.75$  for increasing  $B$ . (e) Fully formed bubbles at  $B/B_{\max} = 1.0$ . (f) The bubble structure expands back toward a uniform state at  $B/B_{\max} = 0.5$  for decreasing  $B$ .

repulsion favors the formation of a uniform triangular lattice, while the attractive term favors bubble formation. For increasing  $B$  at a fixed density, crystal, stripe, and bubble phases appear, while for increasing  $\rho$  at fixed  $B$ , crystal, bubble, stripe, and void lattice phases emerge [32, 44]. The particles are initially placed in random,

non-overlapping positions, and their dynamics evolve according to the overdamped equation

$$\eta \frac{d\mathbf{r}_i}{dt} = - \sum_{j \neq i}^N \nabla V(r_{ij}) \quad (2)$$

The damping term  $\eta = 1.0$ , and we employ a Lekner summation method for computational efficiency in calculating the long-range repulsive term [45, 46]. The strength of the attractive term oscillates with time between  $B = 0.0$  and  $B = B_{\max}$ ,  $B(t) = B_{\max} |\cos(\omega t)|$ . For convenience, we designate one cycle as the progression of  $B$  from  $B = B_{\max}$  to  $B = 0.0$  and back, so that there are two cycles per period  $\tau = 2\pi/\omega$ . In Fig. 1(a), we plot  $V(r_{ij}, t)$  for a system with  $B_{\max} = 2.9$  and  $\omega = 1.25 \times 10^{-4}$  at  $t = \pi n / \omega$ , where  $B = 0.0$  and the interaction is purely repulsive, and at  $t = \pi(n + 1/2) / \omega$ , where  $B = B_{\max}$  and the attractive and repulsive interaction terms are competing. Figure 1(b) shows  $B(t)$  as a function of cycle number  $n$ .

To quantify the behavior, we measure the cumulative displacements of the particles over time,  $d(n) = \sum_i^N |\mathbf{r}_i(t = n) - \mathbf{r}_i(t = 0)|$ , and the net displacement of the particles after a single cycle,  $R(n) = \sum_i^N [\mathbf{r}_i(t = n) - \mathbf{r}_i(t = n - 1)]$ . If the system is in a fluctuating state,  $d(n)$  increases monotonically with time and  $R(n)$  is finite, while in reversible states,  $d(n)$  saturates and  $R(n) \approx 0$ . These are the same measures used in periodically sheared systems to detect R-IR transitions [1-3].

*Results*— In Fig. 1(c) we plot the particle configurations during cycle  $n = 20$  for a system with  $\rho = 0.5$ ,  $B_{\max} = 2.9$ , and  $\omega = 1.25 \times 10^{-4}$  in the  $B/B_{\max} = 0$  portion of the cycle, where a uniform and partially ordered structure appears. During the increasing  $B$  portion of the cycle at  $B/B_{\max} = 0.75$  in Fig. 1(d), the particles are beginning to aggregate into bubbles. Figure 1(e) shows that well defined bubbles are present when  $B/B_{\max} = 1.0$ . As  $B$  decreases again, Fig. 1(f) indicates that at  $B/B_{\max} = 0.5$  the clumps are expanding back toward a uniformly dense state. We note that for  $\rho = 0.5$  at constant  $B$ , the system forms a crystal for  $B \leq 2.0$ , stripes for  $2.0 < B < 2.3$ , and clumps for  $B \geq 2.3$ .

In Fig. 2(a,b), we plot the cumulative displacement  $d(n)$  and displacement per cycle  $R(n)$ , respectively, versus  $n$  for a system with  $\rho = 0.5$  and  $\omega = 1.25 \times 10^{-4}$  at  $B_{\max} = 2.0, 2.4, 2.6, 2.7, 2.8, 2.9, 3.0, 3.2$ , and  $4.0$ . For  $B_{\max} < 2.7$ ,  $d(n)$  saturates to a constant value and  $R(n)$  is close to zero since the system organizes into a reversible state. In contrast, for  $B_{\max} \geq 2.7$ ,  $d(n)$  increases monotonically with  $n$  as  $n^{1/2}$ , the expected behavior for Brownian motion, while  $R(n)$  has a finite value, indicating that the particles do not return to their original positions after each cycle. This behavior of  $d(n)$  and  $R(n)$  is the same as what is found at the R-IR transition in periodically sheared colloidal suspensions [1, 2]. In Fig. 2(c), we show the value of  $R$  after  $n = 200$  cycles versus  $B_{\max}$  for the same system, where we observe a critical amplitude  $B_{\max}^c \approx 2.65$  for the transition to an irreversible state.

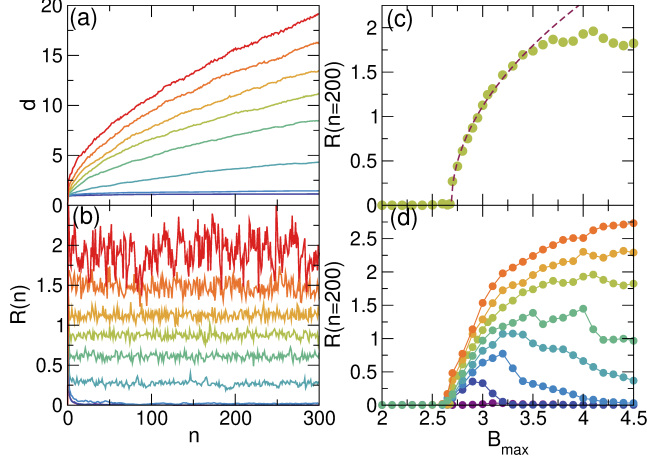


FIG. 2. (a) Cumulative displacements  $d(n)$  vs  $n$  for a system with  $\rho = 0.5$  and  $\omega = 1.25 \times 10^{-4}$  at  $B_{\max} = 2.0, 2.4, 2.6, 2.7, 2.8, 2.9, 3.0, 3.2$ , and  $4.0$ , from bottom to top. (b) The corresponding  $R(n)$  vs  $n$ . The behavior is reversible for  $B_{\max} < 2.7$  and irreversible for  $B_{\max} \geq 2.7$ . (c)  $R$  after  $n = 200$  cycles vs  $B_{\max}$  for the same system, showing a critical transition near  $B_{\max} = 2.65$ . The dashed line is a fit to  $R \propto (B_{\max} - B_{\max}^c)^{\beta}$  with  $B_{\max}^c = 2.69$  and  $\beta = 1/2$ . (d)  $R$  after  $n = 200$  cycles vs  $B_{\max}$  for  $\rho = 0.2, 0.225, 0.25, 0.275, 0.3, 0.35, 0.4, 0.5, 0.6$ , and  $0.8$ , from bottom to top. The lowest three values of  $\rho$  give  $R = 0$  for all  $B_{\max}$ .

The dashed line is a fit to  $R \propto (B_{\max} - B_{\max}^c)^{\beta}$  with  $B_{\max}^c = 2.69$  and  $\beta = 1/2$ . This is the same exponent found by Corte *et al.* [2] for the R-IR transition, and is consistent with the directed percolation universality class [3, 47]. Figure 2(d) shows  $R$  after  $n = 200$  cycles versus  $B_{\max}$  for  $\rho = 0.2, 0.225, 0.25, 0.275, 0.3, 0.35, 0.4, 0.5, 0.6$ , and  $0.8$ . For  $\rho \leq 0.2$  and  $B_{\max} < 2.6$ , the behavior is reversible, indicating that there is both a critical amplitude  $B_{\max}^c$  and a critical density  $\rho_c$  for observing the R-IR transition, similar to what is found in other systems [3]. For  $0.225 \leq \rho \leq 0.35$ , we find a reentrant R-IR transition in which  $R$  is zero for  $B_{\max} < 2.6$ , increases to a nonzero value as  $B_{\max}$  increases, but then drops back to a lower value or to zero at higher  $B_{\max}$ . For densities within this range, R-IR and IR-R transitions occur at two different critical amplitudes  $B_{\max}^{c1, c2}$ .

In Fig. 3(a) we illustrate the particle locations and trajectories during  $n = 5$  cycles in the steady state for a system with  $B_{\max} = 2.9$ ,  $\rho = 0.5$ , and  $\omega = 1.25 \times 10^{-4}$ . The motion is disordered and the behavior is irreversible. At  $\rho = 0.15$  in the same system, shown in Fig. 3(b), we find a reversible state where long-time diffusion is absent and the trajectories are more ordered. In general, particles follow the exact same path during each cycle in the reversible regime, but we find some cases where individual particles return to their original locations after multiple cycles or even undergo an exchange with particles in the same cluster; however, there is no long-time diffusion. The reversible state in Fig. 3(b) can be viewed as an example of a dissipative time crystal, since the over-

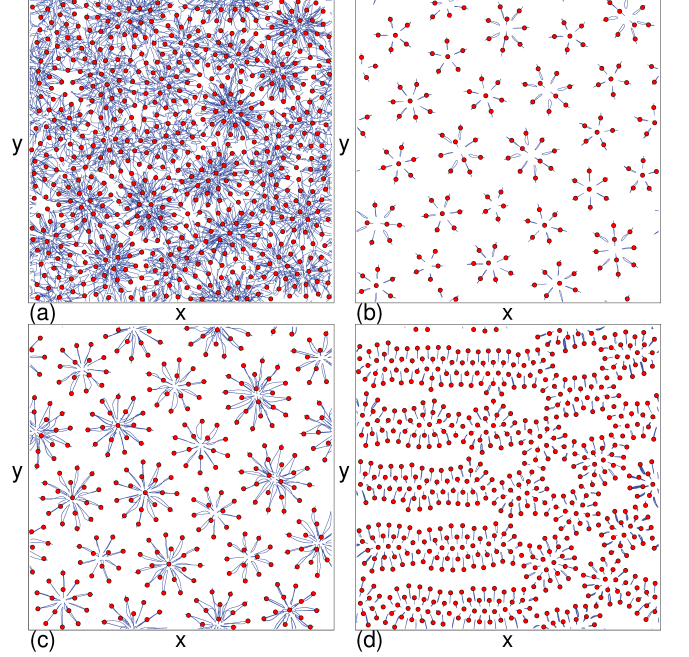


FIG. 3. Particle configurations (red) and trajectories (blue) during  $n = 5$  cycles in the steady state. (a) Disordered flow in the irreversible state at  $\rho = 0.5$ ,  $B_{\max} = 2.9$ , and  $\omega = 1.25 \times 10^{-4}$ . (b) Reversible state at  $\rho = 0.15$ ,  $B_{\max} = 2.9$ , and  $\omega = 1.25 \times 10^{-4}$ . (c) Reentrant reversible state at  $\rho = 0.25$ ,  $B_{\max} = 4.0$ , and  $\omega = 1.25 \times 10^{-4}$ . (d) A stripe-like reversible state at  $\rho = 0.5$  and  $B_{\max} = 3.2$  for a higher frequency of  $\omega = 8.0 \times 10^{-4}$ .

all structure repeats as a function of time [40, 41]. In Fig. 3(c), we show the  $B_{\max} = 4.0$  reentrant reversible state that appears for large  $B_{\max}$  in the  $\rho = 0.25$  system from Fig. 2(d). At this density and oscillation frequency, the repulsion dominates for  $B_{\max} < 2.6$  and the system remains in a uniform distorted crystal state. When  $B_{\max}$  or  $\rho$  increase enough for the system to reach a clump state during the  $B/B_{\max} \approx 1$  portion of the cycle, an irreversible state can emerge in which the system cycles between uniform and clump states. The irreversibility arises if the clumps that form are composed of a different set of particles on each cycle due to mixing that occurs as the system passes in and out of the uniform state, meaning that some particles effectively jump from one clump to another between cycles. At higher  $B_{\max}$ , the clump structure becomes so compact that particles inside the clumps do not have time to fully expand into the uniform crystal state during the decreasing  $B$  portion of the cycle, so each particle becomes confined permanently to a particular clump, as shown for the reentrant reversible state in Fig. 3(c). The R-IR transition is also a function of the oscillation frequency  $\omega$ , and as the frequency varies, a quasi-pattern can emerge in the reversible state, such as the reversible stripe state shown in Fig. 3(d) at  $B_{\max} = 3.2$  and  $\omega = 8.0 \times 10^{-4}$ . If we fix  $B = 3.2$  and do

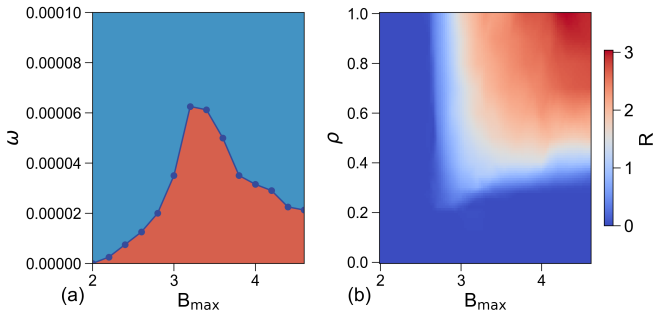


FIG. 4. (a) Boundary between reversible (blue) and irreversible (red) regimes as a function of  $\omega$  vs  $B_{\max}$  for  $\rho = 0.5$ . When  $B_{\max} < 2.0$  and/or at high  $\omega$ , the system is in a reversible uniform state. As a function of  $B_{\max}$  there is a reentrant transition to the reversible state, and the irreversible state reaches its greatest extent near  $B_{\max} = 3.2$ . (b) A heat map of  $R$  after  $n = 200$  cycles as a function of  $\rho$  vs  $B_{\max}$  in a system with  $\omega = 1.25 \times 10^{-4}$  showing reversible (blue) and irreversible (red) regimes.

not oscillate the interaction potential, the system forms a compact bubble state. This indicates that introduction of dynamical oscillation can generate dynamic patterns that would be unstable in a static system.

In Fig. 4(a) we plot the R-IR boundary as a function of  $\omega$  versus  $B_{\max}$  at  $\rho = 0.5$ . There is a reversible state whenever  $\omega$  is large enough that the particles are able to travel a significant distance during an oscillation cycle. For  $B_{\max} < 2.0$ , where the attraction is weak, the reversible configuration is a uniform lattice, and no irreversible behavior occurs even for arbitrarily low  $\omega$ . For  $B_{\max} = 2.6$ , irreversible behavior appears when  $\omega < 1.25 \times 10^{-4}$ , in agreement with the results in Fig. 2(d). As  $B_{\max}$  increases, the reversible transition shifts to larger values of  $\omega$  and reaches a maximum in  $\omega$  at  $B_{\max} = 3.2$ , where at high frequencies, the system forms a reversible stripe state of the type shown in Fig. 3(d). For  $B_{\max} > 3.2$ , the reversible transition drops to lower values of  $\omega$  since, as the particles become more strongly compressed by the attractive portion of the interaction potential, they require more time to expand into a uniform state where irreversible mixing can occur. The reentrant behavior of the reversible state as a function of  $\omega$  is also consistent with the re-entrant behavior observed for varied  $B_{\max}$  at different  $\rho$ , as shown in Fig. 2(d).

Figure 4(b) shows a heat map of  $R$  after  $n = 200$  cycles as a function of  $\rho$  versus  $B_{\max}$  in a system with  $\omega = 1.25 \times 10^{-4}$ . At low  $\rho$  and low  $B_{\max}$ , the system is in a

reversible state. We observe reentrant reversible behavior at higher  $B_{\max}$  when  $\rho$  is not too large. It is possible that additional phases are present within the irreversible regime, such as a state in which particles within a cluster exchange irreversibly but do not leave the cluster, so that there is no long-time diffusion. In general, irreversible behavior arises whenever the combination of  $B_{\max}$ ,  $\omega$ , and  $\rho$  is such that the system can pass through one of the equilibrium phase boundaries, such as bubble to stripe or bubble to uniform, slowly enough that the particles have time to mix.

*Summary*— We have proposed a new type of oscillatory interaction driven non-thermal system that exhibits transitions from reversible states, where there is no long-term diffusion, to irreversible or fluctuating states with finite diffusion. Previous work on reversible-to-irreversible transitions focused on suspensions of particles or amorphous solids subjected to oscillatory shear. Here we consider a pattern-forming system with competing short-range attraction and long-range repulsion, which exhibits uniform crystal, stripe, and bubble states as the ratio of attraction to repulsion is varied. When we oscillate the attractive term, reversible or irreversible behavior appears depending on the amplitude and frequency of the oscillation and the particle density. In the reversible states, it is possible for the particles to undergo complex orbits. The transition to irreversible motion occurs when the system has enough time to relax from the bubble or stripe state into a uniform crystal state during the oscillation period. We show that the reversible motion state can be reentrant as a function of oscillation frequency or maximum attraction amplitude. The reversible states can take the form of dynamic patterns that are not stable in a non-driven system, and these states can be viewed as examples of discrete time crystals. Our results should be general to a broader class of pattern-forming systems with effective competing interactions that can be oscillated as a function of time.

## ACKNOWLEDGMENTS

We gratefully acknowledge the support of the U.S. Department of Energy through the LANL/LDRD program for this work. This work was supported by the US Department of Energy through the Los Alamos National Laboratory. Los Alamos National Laboratory is operated by Triad National Security, LLC, for the National Nuclear Security Administration of the U. S. Department of Energy (Contract No. 892333218NCA000001).

---

[1] D. J. Pine, J. P. Gollub, J. F. Brady, and A. M. Leshansky, Chaos and threshold for irreversibility in sheared suspensions, *Nature (London)* **438**, 997 (2005).

[2] L. Corte, P. M. Chaikin, J. P. Gollub, and D. J. Pine, Random organization in periodically driven systems, *Nature Phys.* **4**, 420 (2008).

[3] C. Reichhardt, I. Regev, K. Dahmen, S. Okuma, and C. J. O. Reichhardt, Reversible to irreversible transitions in periodic driven many-body systems and future directions for classical and quantum systems, *Phys. Rev. Res.*

5, 021001 (2023).

[4] G. I. Menon and S. Ramaswamy, Universality class of the reversible-irreversible transition in sheared suspensions, *Phys. Rev. E* **79**, 061108 (2009).

[5] J. H. Weijs, R. Jeanneret, R. Dreyfus, and D. Bartolo, Emergent hyperuniformity in periodically driven emulsions, *Phys. Rev. Lett.* **115**, 108301 (2015).

[6] E. Tjhung and L. Berthier, Hyperuniform density fluctuations and diverging dynamic correlations in periodically driven colloidal suspensions, *Phys. Rev. Lett.* **114**, 148301 (2015).

[7] Q.-L. Lei and R. Ni, Hydrodynamics of random-organizing hyperuniform fluids, *Proc. Natl. Acad. Sci. (USA)* **116**, 22983 (2019).

[8] S. Wilken, R. E. Guerra, D. J. Pine, and P. M. Chaikin, Hyperuniform structures formed by shearing colloidal suspensions, *Phys. Rev. Lett.* **125**, 148001 (2020).

[9] J. Wang, J. M. Schwarz, and J. D. Paulsen, Propagating irreversibility fronts in cyclically sheared suspensions, *Phys. Rev. Res.* **4**, 013025 (2022).

[10] D. Hexner, P. M. Chaikin, and D. Levine, Enhanced hyperuniformity from random reorganization, *Proc. Natl. Acad. Sci. (USA)* **114**, 4294 (2017).

[11] I. Regev, T. Lookman, and C. Reichhardt, Onset of irreversibility and chaos in amorphous solids under periodic shear, *Phys. Rev. E* **88**, 062401 (2013).

[12] N. C. Keim and P. E. Arratia, Mechanical and microscopic properties of the reversible plastic regime in a 2D jammed material, *Phys. Rev. Lett.* **112**, 028302 (2014).

[13] I. Regev, J. Weber, C. Reichhardt, K. A. Dahmen, and T. Lookman, Reversibility and criticality in amorphous solids, *Nature Commun.* **6**, 8805 (2015).

[14] N. V. Priezjev, Reversible plastic events during oscillatory deformation of amorphous solids, *Phys. Rev. E* **93**, 013001 (2016).

[15] P. K. Jana, M. J. Alava, and S. Zapperi, Irreversibility transition of colloidal polycrystals under cyclic deformation, *Sci. Rep.* **7**, 45550 (2017).

[16] M. O. Lavrentovich, A. J. Liu, and S. R. Nagel, Period proliferation in periodic states in cyclically sheared jammed solids, *Phys. Rev. E* **96**, 020101 (2017).

[17] C. W. Lindeman and S. R. Nagel, Multiple memory formation in glassy landscapes, *Sci. Adv.* **7**, eabg7133 (2021).

[18] N. C. Keim and J. D. Paulsen, Multiperiodic orbits from interacting soft spots in cyclically sheared amorphous solids, *Sci. Adv.* **7**, eabg7685 (2021).

[19] K. Khirallah, B. Tyukodi, D. Vandembroucq, and C. E. Maloney, Yielding in an integer automaton model for amorphous solids under cyclic shear, *Phys. Rev. Lett.* **126**, 218005 (2021).

[20] J. D. Paulsen, N. C. Keim, and S. R. Nagel, Multiple transient memories in experiments on sheared non-Brownian suspensions, *Phys. Rev. Lett.* **113**, 068301 (2014).

[21] D. Fiocco, G. Foffi, and S. Sastry, Encoding of memory in sheared amorphous solids, *Phys. Rev. Lett.* **112**, 025702 (2014).

[22] N. C. Keim, J. D. Paulsen, Z. Zeravcic, S. Sastry, and S. R. Nagel, Memory formation in matter, *Rev. Mod. Phys.* **91**, 035002 (2019).

[23] M. Mungan, S. Sastry, K. Dahmen, and I. Regev, Networks and hierarchies: How amorphous materials learn to remember, *Phys. Rev. Lett.* **123**, 178002 (2019).

[24] J. D. Paulsen and N. C. Keim, Mechanical memories in solids, from disorder to design, *Ann. Rev. Condens. Matter Phys.* **16**, 61 (2025).

[25] N. Mangan, C. Reichhardt, and C. J. O. Reichhardt, Reversible to irreversible flow transition in periodically driven vortices, *Phys. Rev. Lett.* **100**, 187002 (2008).

[26] S. Maeguchi, K. Ienaga, S. Kaneko, and S. Okuma, Critical behavior near the reversible-irreversible transition in periodically driven vortices under random local shear, *Sci. Rep.* **9**, 16447 (2019).

[27] C. Reichhardt and C. J. O. Reichhardt, Reversible to irreversible transitions for cyclically driven particles on periodic obstacle arrays, *J. Chem. Phys.* **156**, 124901 (2022).

[28] D. Minogue, M. R. Eskildsen, C. Reichhardt, and C. J. O. Reichhardt, Reversible, irreversible, and mixed regimes for periodically driven disks in random obstacle arrays, *Phys. Rev. E* **109**, 044905 (2024).

[29] C. J. O. Reichhardt, C. Reichhardt, I. Martin, and A. R. Bishop, Dynamics and melting of stripes, crystals, and bubbles with quenched disorder, *Physica D* **193**, 303 (2004).

[30] K. Nelissen, B. Partoens, and F. M. Peeters, Bubble, stripe, and ring phases in a two-dimensional cluster with competing interactions, *Phys. Rev. E* **71**, 066204 (2005).

[31] Y. H. Liu, L. Y. Chew, and M. Y. Yu, Self-assembly of complex structures in a two-dimensional system with competing interaction forces, *Phys. Rev. E* **78**, 066405 (2008).

[32] C. J. Olson Reichhardt, C. Reichhardt, and A. R. Bishop, Structural transitions, melting, and intermediate phases for stripe- and clump-forming systems, *Phys. Rev. E* **82**, 041502 (2010).

[33] X. B. Xu, H. Fangohr, S. Y. Ding, F. Zhou, X. N. Xu, Z. H. Wang, M. Gu, D. Q. Shi, and S. X. Dou, Phase diagram of vortex matter of type-II superconductors, *Phys. Rev. B* **83**, 014501 (2011).

[34] L. Q. Costa Campos, S. W. S. Apolinario, and H. Löwen, Structural ordering of trapped colloids with competing interactions, *Phys. Rev. E* **88**, 042313 (2013).

[35] Y. Liu and Y. Xi, Colloidal systems with a short-range attraction and long-range repulsion: phase diagrams, structures, and dynamics, *Curr. Opin. Colloid Interf. Sci.* **19**, 123 (2019).

[36] W. Wang, R. Díaz-Méndez, M. Wallin, J. Lidmar, and E. Babaev, Pinning effects in a two-dimensional cluster glass, *Phys. Rev. B* **104**, 144206 (2021).

[37] X. B. Xu, T. Tang, Z. H. Wang, X. N. Xu, G. Y. Fang, and M. Gu, Nonequilibrium pattern formation in circularly confined two-dimensional systems with competing interactions, *Phys. Rev. E* **103**, 012604 (2021).

[38] A. Al Harraq, A. A. Hymel, E. Lin, T. M. Truskett, and B. Bharti, Dual nature of magnetic nanoparticle dispersions enables control over short-range attraction and long-range repulsion interactions, *Commun. Chem.* **5**, 72 (2022).

[39] A. Hooshanginejad, J.-W. Barotta, V. Spradlin, G. Pucci, R. Hunt, and D. M. Harris, Interactions and pattern formation in a macroscopic magnetocapillary salr system of mermaid cereal, *Nature Commun.* **15**, 5466 (2024).

[40] A. Libál, T. Balázs, C. Reichhardt, and C. J. O. Reichhardt, Colloidal dynamics on a choreographic time crystal, *Phys. Rev. Lett.* **124**, 208004 (2020).

[41] N. Y. Yao, C. Nayak, L. Balents, and M. P. Zaletel, Clas-

sical discrete time crystals, *Nature Phys.* **16**, 438 (2020).

[42] A. Ernst, A. M. E. B. Rossi, and T. M. Fischer, Adiabatic and irreversible classical discrete time crystals, *SciPost Phys.* **13**, 091 (2022).

[43] H. Zhao and I. I. Smalyukh, Space-time crystals from particle-like topological solitons, *Nature Mater.* **24**, 1802 (2025).

[44] C. Reichhardt and C. J. O. Reichhardt, Stripe and bubble ratchets on asymmetric substrates, *Phys. Rev. Res.* **6**, 043290 (2024).

[45] J. Lekner, Summation of Coulomb fields in computer-simulated disordered-systems, *Physica A* **176**, 485 (1991).

[46] N. Grønbech-Jensen, Lekner summation of long range interactions in periodic systems, *Int. J. Mod. Phys. C* **8**, 1287 (1997).

[47] H. Hinrichsen, Non-equilibrium critical phenomena and phase transitions into absorbing states, *Adv. Phys.* **49**, 815 (2000).